nature communications

Article

https://doi.org/10.1038/s41467-026-71777-2

The effect of the fitness gradient on fixation probability

Received: 27 June 2025

Accepted: 30 March 2026

Published online: 17 April 2026

Check for updates

Jakub Svoboda[1,2], Hossein Nemati[3], Josef Tkadlec[4], Kamran Kaveh[5] & Krishnendu Chatterjee[1]

Evolutionary biology examines how the genetic and phenotypic composition of populations changes over time. An important goal is to determine the fixation probability of a single advantageous mutant that arises in a homogeneous population of N residents. Many real populations experience environmental gradients that cause mutations to be beneficial in some spatial regions but harmful in others. Here, we study the fixation probability of a mutant placed on a simple one-dimensional spatial structure that experiences such a gradient. The mutant's fitness varies linearly from $1-s$ to $1+s$, whereas the resident fitness is constant and equal to 1. The existing literature suggests that such heterogeneity in the mutant's fitness should lead to a decrease in its fixation probability. However, in this work, we find that small, non-negligible gradients ($s<1/\sqrt{N}$) substantially increase the fixation probability, while larger gradients ($s>(\log N)/\sqrt{N}$) substantially decrease it. Moreover, we quantify the strength of this phenomenon analytically and we precisely delimit the range of the gradients for which it occurs. Our computer simulations closely match those findings. Altogether, our results indicate that subjecting a simple population structure to natural environmental conditions can produce strong counterintuitive effects.

The evolutionary success of a new genotype lies in its ability to establish a new colony and outgrow the competing populations. This depends on several factors. The fitness advantage of a beneficial mutant is often due to genetic (or epigenetic) alterations that equip the individual with a faster reproduction rate or a diminished death rate.

Besides these inherent fitness differences, population structure and environmental factors play a critical role in the outcome of an evolutionary process[1–6]. Evolutionary dynamics in finite population settings have been the subject of much research[3–9]. In finite populations, the stochasticity of the dynamics (often due to random division times or deaths) needs to be taken into account[10]. In these cases, even a neutral or deleterious mutant has a non-zero fixation probability, that is, it may take over the population and wipe out the established resident.

The spatial structure of the population can be described by a graph (network), where each node is occupied by an individual, and the edges (connections) represent the possible interactions or dispersal patterns[1,5]. There has been a lot of focus in the literature on discussing so-called amplifiers of selection, which are graphs that increase the chance of selection of a beneficial mutant[8,9,11–26].

Environmental factors such as distribution of food or other resources across the population also play a critical role in the outcome of an evolutionary process[27–31]. Recently, spatial environmental heterogeneity has been investigated under the framework of evolutionary graphs[32–42]. The idea of 'environmental amplifiers', that is, environmental distributions that increase the fixation probability, is suggested by Maciejweski and Puleo[34] and Kaveh et al.[32]. Interestingly, the condition for selection in two-chromatic graphs[32] can be seen as an evolutionary graph extension of Gillespie's condition for subdivided two-island models[43]. Other aspects of heterogeneity that have been studied include the change in fixation probability and time to fixation in

[1]ISTA, Klosterneuburg, Austria. [2]Dartmouth College, Hanover NH, USA. [3]Utrecht University, Utrecht, Netherlands. [4]Computer Science Institute, Charles University, Prague, Czech Republic. [5]Independent researcher, Toronto, Canada. e-mail: krishnendu.chatterjee@ist.ac.at

random environments[36,37], and condition for coexistence in heterogeneous environments[44].

Perhaps the most relevant example of spatial resource distribution in biological and laboratory settings is the diffusion according to a linear gradient[45–49]. In this scenario, the fitness of the mutants or the residents has an environmental component that is a (linear) function of the distance from the resource. We give three examples. First, in the context of the evolution of drug resistance in microbial populations, competing genotypes are antibiotic-resistant and antibiotic-sensitive strains, as e.g., in the experiments by Baym and Kishony labs, MEGA-plate experiment[46], and Death Galaxy (evolution accelerator) by the Austin lab[50]. The fitness of an antibiotic-sensitive *E. coli* strain increases with the distance from the source of the drug, whereas the fitness of the antibiotic-resistant strain is uniform and equal to some intermediate value[51,52]. Second, in cancer evolution, fitness gradients appear near tumor vasculature where cancer cells are competing with normal tissue cells (or other cancer subtypes). Oxygen and nutrients are constantly diffusing away from the blood vessel into the neighboring cells and thus create a gradient[53]. A third example is the competition between two strains with different metabolic pathways. Each metabolic type consumes a particular sugar. For instance, mutants can digest glucose while residents can only digest lactose (see ref. 54 and references therein). If glucose distribution follows a linear fitness gradient, then only mutants feel the effect of environmental variation, see Fig. 1.

It is suggested that linear gradients can accelerate the process of evolution by allowing faster accumulation of beneficial mutants

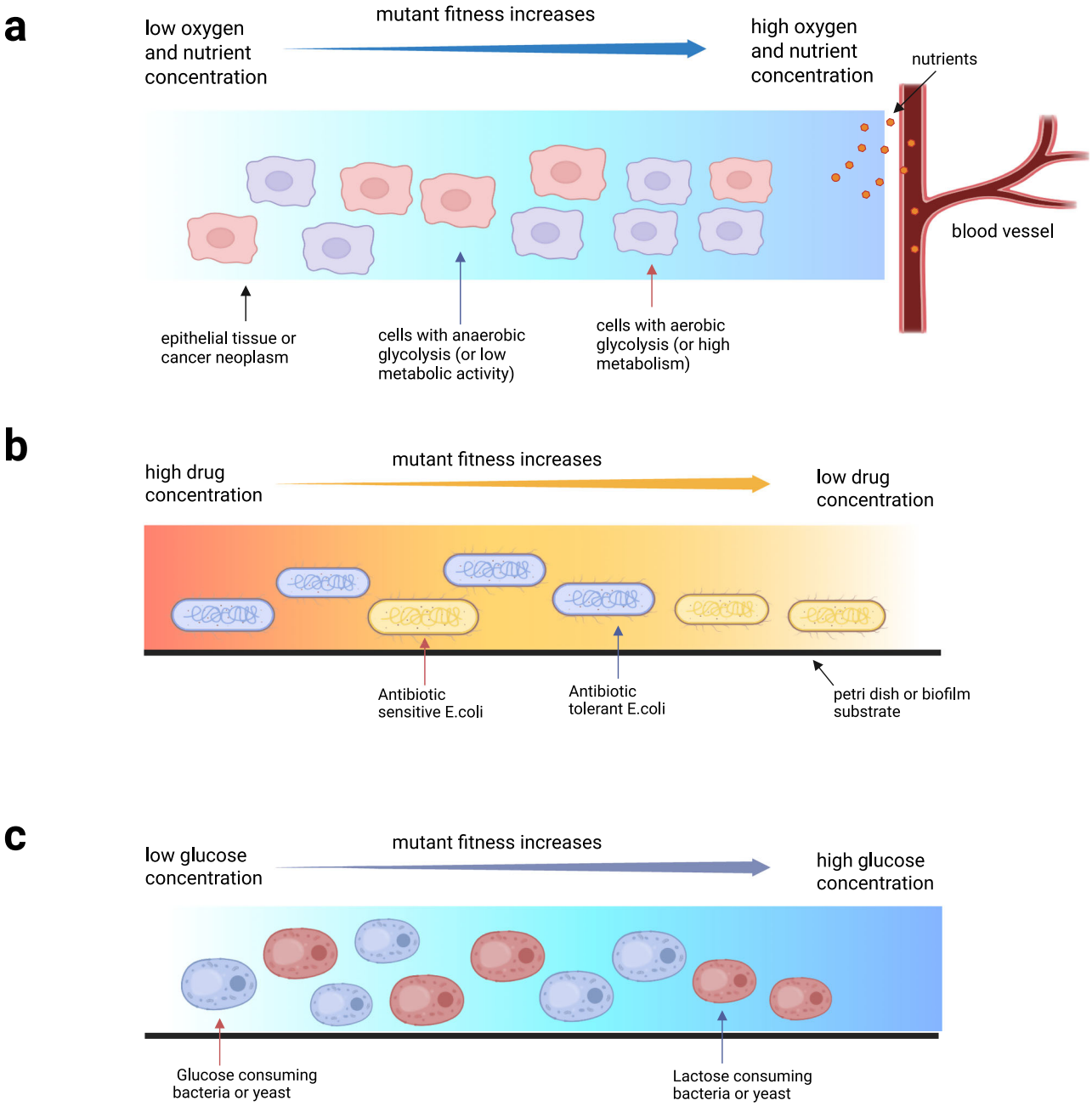

Fig. 1 | Linear fitness gradients. a Example of competition between different cancer phenotypes in nutrient and oxygen gradients near vasculature in the tumor microenvironment. **b** Competition in microbial populations between drug-sensitive (mutant) and drug-resistant strains in an anabiotic gradient. **c** Competition in microbial or yeast populations between two metabolic-specific phenotypes. Resident cells consume lactose with a constant concentration, while glucose-consuming mutants see a gradient of glucose. Created in BioRender. Kaveh, K. (2026) https://BioRender.com/hwyu6gr.

https://doi.org/10.1038/s41467-026-71777-2

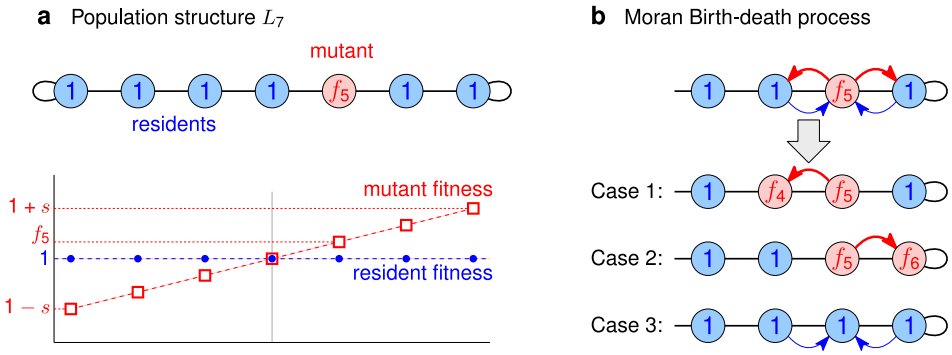

Fig. 2 | Moran process on an isothermal line with mutant fitness gradient. a The spatial structure consists of N nodes arranged along a line L_N. Each node is initially occupied by a resident (blue), except for a single mutant (red). Residents' fitness is normalized to 1, while mutants' fitness $f_1, \ldots, f_N$ is site-specific and varies according to a linear gradient. **b** In a single step of the Moran Birth-death process, a random individual (selected with probability proportional to its fitness) replaces a random neighbor with a copy of itself. Fixation probability is the probability that the mutants eventually take over all the sites.

as the mutant colony grows[55,56]. This is indeed commonly observed in a variety of evolutionary and ecological settings. As heterogeneity increases, it elevates the rate of evolution, that is, the rate of accumulating new mutations, in a mutation-selection process with many allele types[57–59]. A simpler and more fundamental question, however, is the effect of such a linear fitness gradient on the fixation probability of a new mutation. In other words, in a linear graph structure where a resource is linearly increasing across the population, what is the chance of selection of a randomly placed mutant?

To address this question, we consider a population of N individuals arranged along a one-dimensional lattice. The mutants' fitness increases linearly from $1-s$ on the left end to $1+s$ on the right end. The residents' fitness is equal to 1, independent of their position. Thus, the mutants are sensitive to the gradient, whereas the residents are not. The value s is the magnitude of the fitness gradient. The question is how this environmental variation, characterized by the fitness gradient s and the population size N, affects the chance of success of a newly placed mutant.

In the absence of the gradient ($s = 0$), the fixation probability of one randomly placed mutant with no fitness advantage is known to be equal to $\frac{1}{N}$[60]. Moreover, in well-mixed populations, the environmental variations that target the mutant fitness reduce the mutant fixation probability[32]. However, we show that on one-dimensional spatial structures, there exist fitness gradients that substantially increase the fixation probability for a randomly placed mutant.

In this work, we study the fixation probability of a single gradient-sensitive mutant that is invading a background population of insensitive residents. We start by showing numerical results for population sizes $N \le 100$ that illustrate that the fixation probability exhibits intriguing non-monotonic behavior in terms of the gradient s. Namely, small gradients increase the mutant fixation probability, while large gradients decrease it. Next, we analytically characterize the range and the magnitude of those effects for large population sizes N. Our analytical results delineate three regimes that depend on the interplay between the gradient s and the population sizes N. First, we prove that with a negligible gradient (for $s \le \frac{1}{N}$) the fixation probability remains of the order of $\frac{1}{N}$ (Theorem 1). Second, we show that for small (but non-negligible) gradients (for $\frac{1}{N} < s < \frac{1}{\sqrt{N}}$) the fixation probability increases substantially, and becomes of the order of s (Theorem 2). Finally, we show that for large gradients (for $s \gg \frac{1}{\sqrt{N}}$ or $s \ge \frac{\log N}{\sqrt{N}}$) the fixation probability drops drastically and becomes vanishingly small in N (Theorem 3). Overall, our results paint a complete picture of the effect of linear fitness gradients in populations where gradient-sensitive (but otherwise neutral) mutants invade a population of gradient-insensitive residents.

Results

Model

To model the evolutionary dynamics of mutants whose fitness varies linearly with location, we consider a special case of the classic Moran Birth-death process with environmental heterogeneity.

Population structure

We represent the population structure as a graph (network). The N nodes correspond to individual sites, and each edge of the graph corresponds to a possible interaction between individuals occupying those sites. Each site is occupied by a single individual – either a resident or a mutant. Thus, the population size is N. To model an environment that is subject to a linear fitness gradient, we consider a population structure L_N in which the N sites are arranged left to right. Each site is connected to its neighbors along the line. The spatial structure L_N thus represents a one-dimensional lattice. (See also Section 6 in Supplementary Note 1 for results on two-dimensional lattices.) To avoid the boundary effects, we also include self-loops at the two ends. Thanks to this, the resulting graph is isothermal[1], which later simplifies the analysis.

Each individual has some fitness. The fitness of each resident is equal to 1, regardless of which site it occupies. The mutant fitness is site-specific. For convenience, we consider N odd, that is $N = 2 \cdot N_0 + 1$ for some $N_0 \ge 1$. We label the nodes 1, 2, …, N. The mutant fitness f_i at site i is given by a linear expression $1 + s \cdot (i - N_0 - 1)/N_0$, where $s \in [0, 1]$ is the gradient (slope). Note that the average mutant fitness is 1, which is the same as for residents. When $s = 0$ (no gradient), the mutant fitness is equal to 1 at all nodes. For a given gradient $s \in [0, 1]$, the mutant fitness varies from $1 - s$ to $1 + s$. At the extreme $s = 1$, it ranges from 0 to 2. See Fig. 2a.

Moran Birth-death process

The evolutionary dynamic is governed by a standard Moran Birth-death process. Formally, the process occurs in discrete time steps. In each step, first one individual is selected for reproduction, with probability proportional to its fitness. That individual then produces an offspring that migrates along a random adjacent edge and replaces the neighbor. In this way, at most one site may change its status in each step, see Fig. 2b.

Initially, one random site v is occupied by a mutant, and the remaining sites are occupied by residents. Then, the above steps are performed until either all sites are occupied by mutants (we say that fixation occurred) or all sites are occupied by residents (we say that extinction occurred). Given an arbitrary graph G_N with N sites, a mutant fitness gradient s, and the initial mutant location v, the mutant fixation probability is denoted by $\rho(G_N, s, v)$. In the baseline regime $s = 0$ (no gradient), we recover the standard Moran Birth-death process with

https://doi.org/10.1038/s41467-026-71777-2

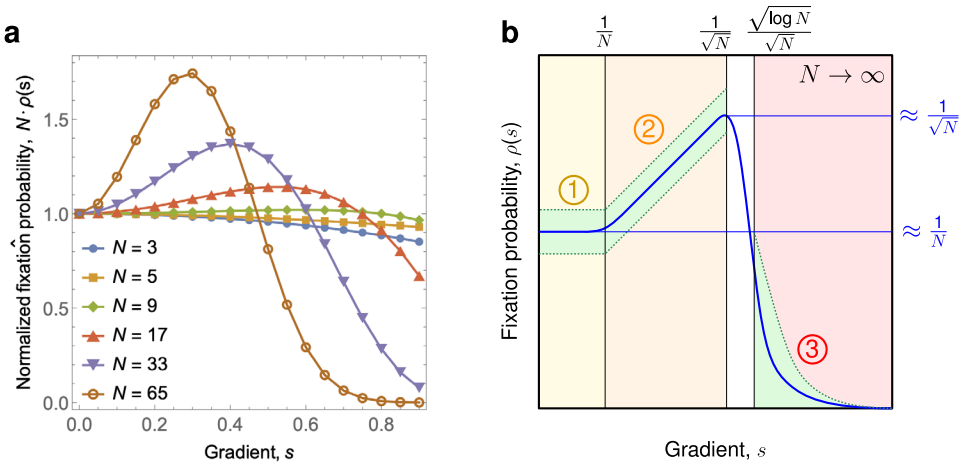

Fig. 3 | Fixation probability $\rho(s)$ on a 1-dimensional lattice L_N, as a function of the gradient s. Recall that with zero gradient ($s = 0$), the normalized fixation probability $N \cdot \rho(0)$ satisfies $N \cdot \rho(0) = 1$ for any population size N. **a** For very small population sizes $N \le 5$, the normalized fixation probability $N \cdot \rho(s)$ slowly decreases as the mutant fitness gradient s increases from $s = 0$ toward $s = 1$. In contrast, for larger $N \ge 9$, it first increases and only then decreases. Here, $N = 2^k + 1$ for $k = 1, \ldots, 6$. **b** In the limit of large population size $N \to \infty$, we show that the fixation probability $\rho(L_N, s)$ scales roughly as $1/N$ when the gradient s is negligible (yellow region, see Theorem 1), then it scales as s when the gradient is small (orange region, see Theorem 2), and finally it drastically drops to 0 when the gradient is too large (red region, see Theorem 3).

neutral mutants. Since our one-dimensional lattice graph L_N is isothermal, we have $\rho(L_N, s = 0, v)$ for any initial mutant location v[1]. (Without self-loops, those fixation probabilities would be $2/(N + 2)$ for mutants who appear at either endpoint of the line, and $1/(N + 2)$ for mutants who appear elsewhere. This would somewhat obscure the comparison, but it would not change the overall trends, compare Fig. 3 and Section 6 in Supplementary Note 1.) When the initial mutant appears at a random location, the (average) fixation probability is denoted by $\rho(G_N, s) = \frac{1}{N}\sum_v \rho(G_N, s, v)$. When G_N coincides with the one-dimensional lattice L_N defined above, and N is clear from the context, we use a shorthand notation $\rho(s) = \rho(L_N, s)$ and $\rho(s, v) = \rho(L_N, s, v)$.

Numerical results

We present two types of results concerning the fixation probability of a single environment-aware mutant who is invading a population of residents who do not perceive the environment.

First, we show numerically that the mutant's fixation probability exhibits intriguing non-monotonic behavior in terms of the gradient s. Second, we show analytically that for large population sizes the magnitude of this effect is substantial (Theorems 2 and 3), unless the gradient s is negligible (Theorem 1).

We consider one-dimensional lattices L_N. For any population size N and any gradient s, the mutant's fixation probability $\rho(L_N, s)$ can be computed numerically by solving a system of 2^N linear equations[61]. However, since the expression 2^N grows exponentially quickly, this approach becomes intractable even for a computer for $N \approx 20$. Fortunately, since the graph L_N has a particularly simple structure, the size of the system can be reduced using standard techniques to roughly N^2 equations[17], which allows us to efficiently compute the fixation probability for larger sizes and for arbitrary gradients s, see Fig. 3a.

For very small population sizes ($N \in \{3, 5\}$), we observe that the fixation probability keeps decreasing as the gradient s increases. This is consistent with a general rule of thumb, which states that in well-mixed populations, heterogeneity in mutant fitness typically decreases the fixation probability of the mutant[32].

In sharp contrast, as the population size grows larger ($N \in \{9, 17, 33, 65\}$), we observe a reversal in this trend. That is, for a certain range of gradients s, the fixation probability of a single mutant invader increases instead of decreasing. However, this effect crucially depends on the magnitude of the gradient. In particular, as the gradient increases, the fixation probability reaches a peak and, upon increasing the gradient further, the fixation probability starts to drop. The same qualitative effects persist for two-dimensional lattices without self-loops, see Section 6 in Supplementary Note 1. When $N = 33$, the peak fixation probability occurs for a gradient of approximately $s \approx 0.4$. At roughly $s \approx 0.6$, the fixation probability drops below the baseline value given by zero gradient, and eventually it falls toward 0.

The numerical approach can also be used to compute the fixation probability $\rho_i = \rho(L_N, s, v_i)$ starting with the initial mutant at a fixed site v_i. When s is large, the fixation probability ρ_i is small, regardless of the initial mutant node v_i.

However, when s is small, then the starting location has a substantial effect. Namely, the fixation probability ρ_i is small for the nodes v_i in the left half, where $f_i < 1$, but it is large for those nodes v_i in the right half, where $f_i > 1$, see Fig. 4.

Informally speaking, starting in the right half is so beneficial to the mutants that it more than compensates for their weak performance when they start in the left half. However, we note that the effect appears only for certain combinations of parameters of the population size N and the gradient s.

Analytical results

In this section, we present our analytical results that explain the surprising non-monotonic behavior in Fig. 3. We show that in the regime of (a) negligible gradient, the fixation probability does not change significantly, (b) small gradient, the fixation probability increases substantially, and (c) large gradient, the fixation probability decreases significantly. First, these results explain the non-monotonic behavior qualitatively, and second, our analytical results also present bounds on the slope, which gives the quantitative characterization of the results and delimits the range of parameters of the phenomenon. The analytical results of the three different regimes are presented below.

Negligible gradient

Recall that when $s = 0$, the fixation probability is known to be equal to $1/N$, where N is the population size. As our first analytical result, we show that, unsurprisingly, negligible gradients do not strongly affect the fixation probability. Formally, we show that when the gradient s is at most $1/N$ (that is, the mutant fitness at any location is sandwiched between $1 - 1/N$ and $1 + 1/N$), then the fixation probability is still of the order of $1/N$.

https://doi.org/10.1038/s41467-026-71777-2

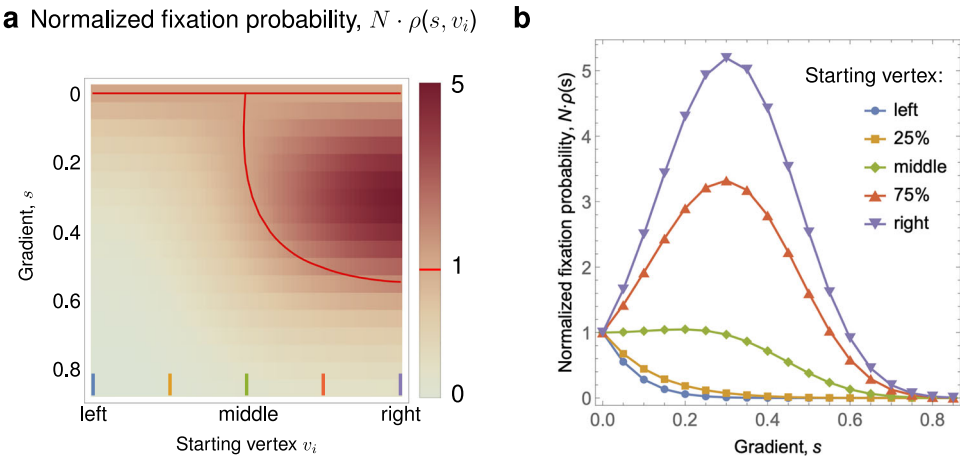

Fig. 4 | The role of the mutant starting vertex v_i. a When $s = 0$ (top row), we have $\rho(s, v_i) = 1/N$ for all initial mutant locations v_i. For other gradients $s > 0$, the fixation probability is the highest when the initial mutant appears at the rightmost vertex. For large gradients, the fixation probability is less than $1/N$, regardless of the starting vertex. **b** For the starting vertex at the left end (blue) or in the middle of the left half (orange), the fixation probability decreases monotonically with the slope. For the other starting vertices (middle, middle of the right half, right end), it first increases and then decreases. Here $N = 65$.

Theorem 1. Let $0 \le s \le 1/N$. Then

$$\frac{1}{2N} \le \rho(L_N, s) \le \frac{2}{N}. \tag{1}$$

It is clear that a result of this form must hold for all sufficiently small gradients s; it is perhaps not a priori clear that "sufficiently small" includes $s = 1/N$, that is, regimes when the mutant fitness varies from $1 - 1/N$ up to $1 + 1/N$.

The intuition behind the proof is that the fixation probability can be written as a certain sum that involves terms of the form s^N. For $s \le 1/N$, we can use a known limit $\lim_{N\to\infty}(1+1/N)^N = e \doteq 2.718 < 3$ to bound such terms by constants. This, in turn, bounds the magnitude of the effect of the gradient on the fixation probability. See Supplementary Note 1 for details.

Small gradient

As our main theoretical result, we show that when the population size N is large, a certain value of the gradient s substantially increases the mutant fixation probability, as compared to the baseline case of no gradient.

Theorem 2. Let $\frac{1}{N} \le s \le \frac{3}{4}N^{-\frac{1}{2}}$, then

$$\frac{1}{500}s \le \rho(L_N, s) \le 2s. \tag{2}$$

Our first result (Theorem 1) shows that with negligible fitness gradients $s \le \frac{1}{N}$, the mutant fixation probability decays inversely proportionally with respect to the population size N. In contrast, when the gradient is in the range $\frac{1}{N} \ll s \ll \frac{1}{\sqrt{N}}$, Theorem 2 states that the fixation probability is asymptotically equal to s. In particular, for $s^* = \frac{1}{2\sqrt{N}}$ the fixation probability $\rho(L_N, s^*)$ decays as $1/\sqrt{N}$, so for large N it is substantially larger than $1/N$. Thus, contrary to the common rule of thumb[32], mutant fitness heterogeneity may lead to an increase in the mutant fixation probability. We note that this is consistent with the findings reported in Fig. 3. Moreover, we note that, as N grows large, the ratio of the two fixation probabilities $\rho(L_N, s^*)$ and $\rho(L_N, s = 0)$ tends to infinity; thus, the increase is substantial.

The intuitive idea behind the proof of Theorem 2 is to show that with gradient s in this range, a mutant starting close to the rightmost end of the line has a high chance of fixating. Our bounds on "close" and "high" are strong enough to guarantee that even if all other mutant starting locations always led to mutant extinction, the average fixation probability would still be sufficiently high. See Supplementary Note 1 for details.

Large gradient

Theorem 2 suggests that the steeper the gradient, the higher the fixation probability. As our third analytical result, we show that once the gradient s exceeds the value $\frac{1}{\sqrt{N}}$ by a logarithmic factor, the fixation probability becomes substantially smaller than the reference value $1/N$. In fact, we present a bound that can be adjusted by selecting a suitable value of parameter $k \ge 1$.

Theorem 3. Let $s \ge \sqrt{20\frac{(k+1)\log N}{N}}$, then

$$\rho(L_N, s) \le \frac{1}{N^k}. \tag{3}$$

Thus, increasing the gradient well beyond the threshold of $s = \frac{1}{\sqrt{N}}$ ceases to help the mutants and instead causes their fixation probability to quickly drop towards 0 (rather than decaying proportionally to s, or inversely proportionally to the population size). This is again consistent with the findings reported in Fig. 3.

The intuitive idea behind the proof of Theorem 3 is to show that when the slope is too large, the disadvantage that the mutants perceive near the left endpoint of the line is much more severe than the advantage they perceive near the right endpoint of the line. (Mathematically, this turns out to be a consequence of an inequality $(1 - q)(1 + q) < 1$ which holds for any $q \in (0, 1)$.) Thus, even when the initial mutant appears near the right endpoint and gives rise to a non-negligible mutant subpopulation, that subpopulation is more likely to eventually go extinct than it is to take over the sites near the left endpoint. See Supplementary Note 1 for details.

Discussion

Populations evolve in heterogeneous environments. Concentrations of various chemicals (nutrients or antibiotics) might cause a newly occurring mutation to be beneficial in one spatial region, while being deleterious in another region. In this work, we study possibly the simplest non-trivial case of this general phenomenon, in which the mutant fitness varies according to a linear gradient, whereas the resident fitness is constant.

Table 1 | Overview of results on environmental heterogeneity in structured populations

Population Structure	Change due to heterogeinity	Reference	Technique
Well-mixed	$\rho_A\downarrow$	32	Martingale analysis
Two-island	$\rho_A\uparrow$	28,29	Fokker-Planck equation
Line with fitness gradient	$\rho_A\uparrow$ then $\rho_A\downarrow$	This work	Markov Chain analysis

Apart from the population size N, we thus introduce a single new parameter $s \in (0, 1)$ that parametrizes the steepness of the gradient. That is, the mutant fitness varies linearly from $1 - s$ to $1 + s$, depending on its location within the population. The resident fitness is equal to 1 everywhere. Thus, when averaged over the whole population, the mutant and the resident fitness are equal. Our main quantity of interest is the fixation probability of the mutant who perceives the fitness gradient s.

Even in this simple scenario, we find an intriguing non-monotonic dependence of the fixation probability on s. Earlier research, presented in Table 1, indicated that, as a rule of thumb, mutant fitness heterogeneity in large populations has a monotonic effect on the fixation probability. For well-mixed populations, mutant fitness heterogeneity decreases the fixation probability[32], while for two-island graphs it increases the fixation probability[28,29]. In contrast, here we identify a regime of small but non-negligible gradients s that substantially increase the fixation probability, whereas too high a gradient decreases it. Moreover, for large population sizes, we analytically delimit both the range of gradients for which the increase occurs, as well as the magnitude of the increase. It turns out that the increase is the most prominent when s is of the order of $\frac{1}{\sqrt{N}}$, in which case the fixation probability increases from roughly $\frac{1}{N}$ to roughly $\frac{1}{\sqrt{N}}$, see Theorem 2. We also show that upon further increasing the gradient, the fixation probability abruptly drops and becomes substantially smaller than the baseline value of $1/N$, see Theorem 3. In some ways, this threshold behavior is akin to the threshold $s \cdot N \approx 1$ that separates the weak and strong selection in the case of homogeneous environments in which mutants have a constant fitness advantage.

As mentioned in the introduction, the setting where only mutants perceive the environmental variations is biologically relevant. For example, it is a question of what conditions drug-sensitive microbial strains can have a finite chance to take over a resident drug-resistant population. Our findings suggest that carefully calibrated small environmental gradients can, in fact, increase the chance of selection of the drug-sensitive mutants. Our results show that this is the case even when the cost of resistance is negligible, that is, when mutants and residents are neutral relative to each other in the absence of environmental variations.

Another example would be competition between two metabolically distinct prokaryotic strains, where each strain consumes a particular nutrient. For instance, consider two strains of E. coli where the residents consume glucose and the mutants consume lactose. Suppose that lactose has a linear distribution across the population, while glucose concentration is kept uniform. For gentle gradients of lactose concentration, we expect an emergence of new metabolic phenotypes, whereas for steeper gradients, we expect the resident glucose-consuming strain to remain dominant.

In our analysis, we intentionally focused on perhaps the simplest non-trivial setting of environmental heterogeneity. In particular, we concentrated on the regime in which the fitness gradient is linear, the mutants are gradient-sensitive, and the residents are not. Moreover, we considered a specific linear spatial structure (see also Section 6 in Supplementary Note 1 for two-dimensional lattices), and we assumed that the average mutant fitness is the same as the resident fitness, which gave us a clean baseline $1/N$ for the fixation probability. Analyzing the other settings in which some of the above assumptions are altered or relaxed is an interesting area for future work.

Methods

We use the Moran Birth-death process as described above in Sections "Population structure" and "Moran Birth-death process". Our numerical results are obtained by solving the underlying Markov chain. See Supplementary Note 1 for details.

Data availability

The data generated in this study have been deposited in the Figshare database under accession code https://doi.org/10.6084/m9.figshare.29271674.

Code availability

The related computer code has been deposited in the Figshare database under the accession code https://doi.org/10.6084/m9.figshare.29271674.

References

1. Nowak, M. A. *Evolutionary Dynamics: Exploring The Equations of Life* (Harvard University Press, 2006).
2. Broom, M. & Rychtár, J. *Game-Theoretical Models in Biology* (CRC Press, 2014).
3. Ewens, W. J. *Mathematical Population Genetics: Theoretical Introduction*, Vol. 27 (Springer, 2004).
4. Traulsen, A. & Hauert, C. Stochastic evolutionary game dynamics. *Rev. Nonlinear Dyn. Complex.* **2**, 25–61 (2009).
5. Lieberman, E., Hauert, C. & Nowak, M. A. Evolutionary dynamics on graphs. *Nature* **433**, 312–316 (2005).
6. Allen, B. et al. Evolutionary dynamics on any population structure. *Nature* **544**, 227–230 (2017).
7. Kimura, M. *Population Genetics, Molecular Evolution, and the Neutral Theory: Selected Papers* (University of Chicago Press, 1994).
8. Maruyama, T. On the fixation probability of mutant genes in a subdivided population. *Genet. Res.* **15**, 221–225 (1970).
9. Allen, B. et al. The molecular clock of neutral evolution can be accelerated or slowed by asymmetric spatial structure. *PLoS Comput. Biol.* **11**, e1004108 (2015).
10. Durrett, R. & Levin, S. The importance of being discrete (and spatial). *Theor. Popul. Biol.* **46**, 363–394 (1994).
11. Maruyama, T. A Markov process of gene frequency change in a geographically structured population. *Genetics* **76**, 367–77 (1974).
12. Maruyama, T. A simple proof that certain quantities are independent of the geographical structure of population. *Theor. Popul. Biol.* **5**, 148–54 (1974).
13. Komarova, N. Spatial stochastic models for cancer initiation and progression. *Bull. Math. Biol.* **68**, 1573–1599 (2006).
14. Hindersin, L. & Traulsen, A. Counterintuitive properties of the fixation time in network-structured populations. *J. R. Soc. Interface* **11**, 20140606 (2014).
15. Hindersin, L. & Traulsen, A. Most undirected random graphs are amplifiers of selection for birth-death dynamics, but suppressors of selection for death-birth dynamics. *PLoS Comput. Biol.* **11**, e1004437 (2015).
16. Broom, M., Rychtář, J. & Stadler, B. Evolutionary dynamics on graphs-the effect of graph structure and initial placement on mutant spread. *J. Stat. Theory Pract.* **5**, 369–381 (2011).

17. Broom, M. & Rychtář, J. An analysis of the fixation probability of a mutant on special classes of non-directed graphs. *Proc. R. Soc. A* **464**, 2609–2627 (2008).
18. Monk, T., Green, P. & Paulin, M. Martingales and fixation probabilities of evolutionary graphs. *Proc. R. Soc. A* **470**, 20130730 (2014).
19. Houchmandzadeh, B. & Vallade, M. Alternative to the diffusion equation in population genetics. *Phys. Rev. E* **82**, 051913 (2010).
20. Houchmandzadeh, B. & Vallade, M. The fixation probability of a beneficial mutation in a geographically structured population. *N. J. Phys.* **13**, 073020 (2011).
21. Kaveh, K., Komarova, N. L. & Kohandel, M. The duality of spatial death–birth and birth–death processes and limitations of the isothermal theorem. *R. Soc. Open Sci.* **2**, 140465 (2015).
22. Tkadlec, J., Pavlogiannis, A., Chatterjee, K. & Nowak, M. A. Population structure determines the tradeoff between fixation probability and fixation time. *Commun. Biol.* **2**, 138 (2019).
23. Pavlogiannis, A., Tkadlec, J., Chatterjee, K. & Nowak, M. A. Amplification on undirected population structures: comets beat stars. *Sci. Rep.* **7**, 82 (2017).
24. Pavlogiannis, A., Tkadlec, J., Chatterjee, K. & Nowak, M. A. Construction of arbitrarily strong amplifiers of natural selection using evolutionary graph theory. *Commun. Biol.* **1**, 71 (2018).
25. Adlam, B., Chatterjee, K. & Nowak, M. A. Amplifiers of selection. *Proc. R. Soc. A* **471**, 20150114 (2015).
26. Svoboda, J., Joshi, S., Tkadlec, J. & Chatterjee, K. Amplifiers of selection for the Moran process with both birth-death and death-birth updating. *PLOS Comput. Biol.* **20**, e1012008 (2024).
27. Levins, R. Theory of fitness in a heterogeneous environment. i. the fitness set and adaptive function. *Am. Nat.* **96**, 361–373 (1962).
28. Whitlock, M. C. & Gomulkiewicz, R. Probability of fixation in a heterogeneous environment. *Genetics* **171**, 1407–1417 (2005).
29. Gavrilets, S. & Gibson, N. Fixation probabilities in a spatially heterogeneous environment. *Popul. Ecol.* **44**, 51–58 (2002).
30. Vuilleumier, S., Goudet, J. & Perrin, N. Evolution in heterogeneous populations: from migration models to fixation probabilities. *Theor. Popul. Biol.* **78**, 250–258 (2010).
31. Schreiber, S. J. & Lloyd-Smith, J. O. Invasion dynamics in spatially heterogeneous environments. *Am. Nat.* **174**, 490–505 (2009).
32. Kaveh, K., McAvoy, A. & Nowak, M. A. Environmental fitness heterogeneity in the Moran process. *R. Soc. Open Sci.* **6**, 181661 (2019).
33. Kaveh, K., McAvoy, A., Chatterjee, K. & Nowak, M. A. The Moran process on 2-chromatic graphs. *PLOS Comput. Biol.* **16**, e1008402 (2020).
34. Maciejewski, W. & Puleo, G. J. Environmental evolutionary graph theory. *J. Theor. Biol.* **360**, 117–128 (2014).
35. Giaimo, S., Arranz, J. & Traulsen, A. Invasion and effective size of graph-structured populations. *PLoS Comput. Biol.* **14**, e1006559 (2018).
36. Mahdipour-Shirayeh, A., Darooneh, A., Long, A., Komarova, N. & Kohandel, M. Genotype by random environmental interactions gives an advantage to non-favored minor alleles. *Sci. Rep.* **7**, 1–8 (2017).
37. Farhang-Sardroodi, S., Darooneh, A. H., Nikbakht, M., Komarova, N. L. & Kohandel, M. The effect of spatial randomness on the average fixation time of mutants. *PLoS Comput. Biol.* **13**, e1005864 (2017).
38. Farhang-Sardroodi, S., Darooneh, A. H., Kohandel, M. & Komarova, N. L. Environmental spatial and temporal variability and its role in non-favoured mutant dynamics. *J. R. Soc. Interface* **16**, 20180781 (2019).
39. Masuda, N., Gibert, N. & Redner, S. Heterogeneous voter models. *Phys. Rev. E* **82**, 010103 (2010).
40. Hauser, O. P., Traulsen, A. & Nowak, M. A. Heterogeneity in background fitness acts as a suppressor of selection. *J. Theor. Biol.* **343**, 178–185 (2014).
41. Nemati, H., Kaveh, K. & Ejtehadi, M. R. Counterintuitive properties of evolutionary measures: a stochastic process study in cyclic population structures with periodic environments. *J. Theor. Biol.* **564**, 111436 (2023).
42. Brewster, D. A. et al. Maintaining diversity in structured populations. *PNAS Nexus* **4**, pgaf252 (2025).
43. Gillespie, J. H. Natural selection for variances in offspring numbers: a new evolutionary principle. *Am. Nat.* **111**, 1010–1014 (1977).
44. Svoboda, J., Tkadlec, J., Kaveh, K. & Chatterjee, K. Coexistence times in the Moran process with environmental heterogeneity. *Proc. R. Soc. A* **479**, 20220685 (2023).
45. Stevanovic, M. et al. Nutrient gradients mediate complex colony-level antibiotic responses in structured microbial populations. *Front. Microbiol.* **13**, 740259 (2022).
46. Baym, M. et al. Spatiotemporal microbial evolution on antibiotic landscapes. *Science* **353**, 1147–1151 (2016).
47. Altay, G. et al. Modeling biochemical gradients in vitro to control cell compartmentalization in a microengineered 3d model of the intestinal epithelium. *Adv. Healthc. Mater.* **11**, 2201172 (2022).
48. Minchinton, A. I. & Tannock, I. F. Drug penetration in solid tumours. *Nat. Rev. Cancer* **6**, 583–592 (2006).
49. Müller, M., dela Pena, A. & Derendorf, H. Issues in pharmacokinetics and pharmacodynamics of anti-infective agents: distribution in tissue. *Antimicrob. Agents Chemother.* **48**, 1441 (2004).
50. Wu, A., Liao, D., Tlsty, T. D., Sturm, J. C. & Austin, R. H. Game theory in the death galaxy: interaction of cancer and stromal cells in tumour microenvironment. *Interface Focus* **4**, 20140028 (2014).
51. Andersson, D. I. & Hughes, D. Antibiotic resistance and its cost: is it possible to reverse resistance? *Nat. Rev. Microbiol.* **8**, 260–271 (2010).
52. Melnyk, A. H., Wong, A. & Kassen, R. The fitness costs of antibiotic resistance mutations. *Evolut. Appl.* **8**, 273–283 (2015).
53. Wu, A. et al. Cell motility and drug gradients in the emergence of resistance to chemotherapy. *Proc. Natl. Acad. Sci. USA* **110**, 16103–16108 (2013).
54. Lambert, G. & Kussell, E. Memory and fitness optimization of bacteria under fluctuating environments. *PLoS Genet.* **10**, e1004556 (2014).
55. Hermsen, R., Deris, J. B. & Hwa, T. On the rapidity of antibiotic resistance evolution facilitated by a concentration gradient. *Proc. Natl. Acad. Sci. USA* **109**, 10775–10780 (2012).
56. Greulich, P., Waclaw, B. & Allen, R. J. Mutational pathway determines whether drug gradients accelerate evolution of drug-resistant cells. *Phys. Rev. Lett.* **109**, 088101 (2012).
57. Kepler, T. B. & Perelson, A. S. Drug concentration heterogeneity facilitates the evolution of drug resistance. *Proc. Natl. Acad. Sci. USA* **95**, 11514–11519 (1998).
58. Moreno-Gamez, S. et al. Imperfect drug penetration leads to spatial monotherapy and rapid evolution of multi-drug resistance. *bioRxiv* https://doi.org/10.1101/013003 (2014).
59. Fu, F., Nowak, M. A. & Bonhoeffer, S. Spatial Heterogeneity in Drug Concentrations Can Facilitate the Emergence of Resistance to Cancer Therapy. *PLoS Comput. Biol.* **11**, e1004142 (2015).
60. Moran, P. A. P. Random processes in genetics. In *Mathematical Proc. Cambridge Philosophical Society*, Vol. 54, 60–71 (Cambridge University Press, 1958).
61. Hindersin, L., Wu, B., Traulsen, A. & García, J. Computation and simulation of evolutionary game dynamics in finite populations. *Sci. Rep.* **9**, 6946 (2019).

Acknowledgements

J.S. and K.C. were supported by the European Research Council (ERC) CoG 863818 (ForM-SMArt) and Austrian Science Fund (FWF) 10.55776/COE12. J.T. was supported by GAČR grant 25-17377S and by Charles Univ. projects UNCE 24/SCI/008 and PRIMUS 24/SCI/012.

Author contributions

Conceptualization: H.N., K.K., and K.C. Investigation: J.S., H.N., J.T., K.K., and K.C. Visualization: H.N., J.T., and K.K. Formal analysis: J.S., J.T. Project administration: K.K., K.C. Writing–original draft: J.S., H.N., J.T., K.K., and K.C. Writing–editing: J.S., H.N., J.T., K.K., and K.C.

Competing interests

The authors declare no competing interests.

Additional information

Supplementary information The online version contains supplementary material available at https://doi.org/10.1038/s41467-026-71777-2.

Correspondence and requests for materials should be addressed to Krishnendu Chatterjee.

Peer review information *Nature Communications* thanks the anonymous reviewers for their contribution to the peer review of this work. A peer review file is available.